

1 Extreme storms during the last 6,500 years from lagoonal  
2 sedimentary archives in Mar Menor (SE SPAIN)

3  
4  
5  
6 Dezileau L. <sup>\*</sup> <sup>1</sup>, Pérez-Ruzafa A. <sup>2</sup>, Blanchemanche P. <sup>3</sup>, Degeai J.P. <sup>3</sup>, Raji O. <sup>1,4</sup>,  
7 Martinez P. <sup>5</sup>, Marcos C. <sup>2</sup> and Von Grafenstein U. <sup>6</sup>

8  
9  
10 [1]{Université de Montpellier, Geosciences Montpellier, CNRS, UMR 5243}

11 [2]{Universidad de Murcia, Departamento de Ecología e Hidrología, Regional Campus of International Excellence  
12 Campus Mare Nostrum, Murcia 30100, Spain}

13 [3]{Université Montpellier 3, Laboratoire d'Archéologie des Sociétés Méditerranéennes, CNRS, UMR 5140}

14 [4]{Department of Earth Sciences, Université MohammedV-Agdal, Rabat, Morocco}

15 [5]{Université Bordeaux 1, EPOC, CNRS, UMR 5805}

16 [6]{Laboratoire des Sciences du Climat et de l'Environnement, CNRS/CEA, Saclay}

17  
18  
19 \* Correspondence to : laurent.dezileau@gm.univ-montp2.fr  
20

21

## 22 **Abstract**

23 Amongst the most devastating marine catastrophes that can occur in coastal areas, are storms and  
24 tsunamis, which may seriously endanger human society. Many such events are known and have  
25 been reported for the Mediterranean, a region where high-frequency occurrences of these extreme  
26 events coincides with some of the most densely populated coastal areas in the world. In a  
27 sediment core from Mar Menor Lagoon (SE Spain), we discovered eight coarse grained layers  
28 which document marine incursions during periods of intense storm activity or tsunami events.  
29 Based on radiocarbon dating, these extreme events occurred around 5250, 4000, 3600, 3010,  
30 2300, 1350, 650 and 80 years cal BP. No comparable events have been observed during the 20<sup>th</sup>  
31 and 21<sup>th</sup> centuries. The results indicate little likelihood of a tsunami origin for these coarse grained  
32 layers, although historical tsunami events are recorded in this region. These periods of surge  
33 events seem to coincide with the coldest periods in Europe during the late Holocene, suggesting a  
34 control by a climatic mechanism for periods of increased storm activity. Spectral analyses  
35 performed on the sand % revealed four major periodicities of  $1228 \pm 327$ ,  $732 \pm 80$ ,  $562 \pm 58$ , and  
36  $319 \pm 16$  yr. Amongst the well-known proxies that have revealed a millennial-scale climate  
37 variability during the Holocene, the ice-rafted debris (IRD) indices in North Atlantic developed  
38 by Bond et al. (1997, 2001) present a cyclicity of  $1470 \pm 500$  yr, which matches the  $1228 \pm 327$  yr  
39 periodicity evidenced in the Mar Menor lagoon, considering the respective uncertainties on the  
40 periodicities. Thus, an in-phase storm activity in Western Mediterranean is found with the coldest  
41 periods in Europe and to the North Atlantic thermohaline circulation. However, further  
42 investigations, such as additional coring, high-resolution coastal imagery, are needed to better

43 constrain the main cause of these multiple-events.

44

45

46

47 Keywords: coastal lagoons, storm, tsunami, Mediterranean Sea, Late Holocene.

48

49

## 50 1. Introduction

51 In the last century the Mediterranean coastal zones have undergone a considerable development  
52 and the coastal disasters incidence has significantly increased. The coastal zones are exposed to  
53 flooding and coastal erosion processes, and are highly vulnerable to extreme events, such as  
54 storms, cyclones or tsunamis, that can cause significant losses (Seisdedos et al., 2013).

55 Mediterranean intense storms and cyclones are rare meteorological phenomena observed in the  
56 Mediterranean Sea. Different climatological and meteorological works in the western  
57 Mediterranean area show that extreme storms and cyclones show a complex variability in the  
58 sense of non-uniform spatial and temporal patterns (Trigo et al., 2000; Lionello et al., 2006;  
59 Gaertner et al., 2007). This is in partly due to the lack of a clear large scale pattern which may be  
60 expected when dealing with intense events, as the number of events is low with irregular intensity  
61 and intervals. More long-term observations or palaeo-reconstructions in different areas of the  
62 western Mediterranean are needed. Tsunamis are known to occur in the Mediterranean Sea where  
63 all types of sources earthquakes, volcanic eruptions and landslides from the continental margins  
64 are active. There are evidences of large tsunamis during the historical and pre-historical period,  
65 especially in the tectonically more active eastern Mediterranean (e.g., Kelletat and Schellmann,

66 2002; Morhange et al., 2006). The western part of the basin has also been reported as tsunami-  
67 exposed. Historic events have been reported from the Algerian coast and tsunami propagation has  
68 been modelled (Alvarez-Gomez et al., 2011). Geomorphic evidence of ancient tsunami impacts  
69 has also been documented (Maouche et al., 2009). A long-term record of tsunami and storm  
70 activity on time scales of centuries to millennia is especially important in understanding the  
71 temporal variability of these extreme events.

72

73 This study focuses mainly on the Murcia province in Spain (Figure 1). This lowland  
74 Mediterranean coast is sensitive to risks of submersion during extreme events. We propose to use  
75 a high-resolution geochemical and sedimentological approach to reconstruct past surge events in  
76 the Mar Menor lagoon, and then confront our results with extreme historical coastal events in the  
77 western Mediterranean.

78

## 79 2. Study site

80

81 The Mar Menor lagoon is the largest lagoon on the Spanish Mediterranean coast, located at the  
82 SE of the Iberian Peninsula, in the region of Murcia in the area called Campo de Cartagena basin  
83 (Lat. 37.786129, Lon. 0.810450, Figure 1). This coastal lagoon occupies an area of  
84 approximately 135 km<sup>2</sup> with an average depth of 3.6 m. This lagoon is separated from the  
85 Mediterranean sea by La Manga, which is a sandy barrier of 20 km long, between 30 and 500 m  
86 wide and less than 3 m above sea level. This sandy barrier is crossed by five, more or less  
87 functional, channels or “golas”. The Campo de Cartagena Basin represent 1,440 km<sup>2</sup>, with an  
88 elevations ranging from the sea level to 1065 m, surrounded by the Mediterranean Sea to the

89 East, the anticline of Torrevieja to the North and the Cartagena-La Unión mountain range to the  
90 south. This basin is filled by sediments from early Miocene to Quaternary. The major lithologies  
91 are composed of sand, silt, clay conglomerate, caliche and sandstone of the Quaternary period;  
92 marl, conglomerate and gypsum for the Miocene and Pliocene periods (Jiménez-Martínez et al.,  
93 2012). The lagoon and the northern salt marshes of San Pedro are protected for their ecological  
94 importance (Special Protected Area of Mediterranean Interest, Natura 2000 network and  
95 Ramsar). The area is impacted by residual past mining activity, agricultural activities (intensive  
96 fruits and vegetable production), and urban growth coupled with touristic development since  
97 1956 (Pérez-Ruzafa et al., 1987; 1991; 2005). Most of La Manga area is urbanized, a population  
98 of 10,000 inhabitants live here all year long, and growing to ~ 200,000 habitants during summer.  
99 High population density and low level topography makes the area very sensitive to the impact of  
100 climate change and sea level rise. Mar Menor lagoon is considered as one of the Spanish coast  
101 most threatened site by the mean sea level rise and possible increase of extreme climatic events.

102

103

### 104 3. Materials and methods

105

#### 106 3.1 Core material

107

108 A 4-m-long piston core (MM2) was collected in the Mar Menor lagoon in September 2011  
109 (Figure 1) with the UWITEC<sup>®</sup> gravity coring platform (Laboratoire des Sciences du Climat et de  
110 l'Environnement and University of Chambéry) using a simplified piston corer of 2 m length and  
111 83 mm inner diameter. Two consecutive sections (0 to 2 m and 2 to 4m sediment depth,

112 respectively, were cored from a first position followed by a third section (1 to 3m) from a  
113 position ca 1 m apart to cover the technical hiatus between the first two sections. MM2 core was  
114 collected at 4 m below sea level.

115

### 116 3.2 Physical measures

117

118 Back to the laboratory, the structure of the sediment was studied using the Scopix X-ray scanning  
119 (EPOC, University of Bordeaux 1) and photographed. This was complemented by granulometric  
120 analyses on contiguous 1-cm samples using a Beckman-Coulter LS13320 laser diffraction  
121 particle-size analyser (Géosciences Montpellier). XRF analysis were performed on the surface of  
122 split sediment core MM2 every 0.5 cm using a non-destructive Avaatech core-scanner (EPOC,  
123 Université Bordeaux 1). The split core was covered with a 4  $\mu\text{m}$  thin Ultralene to avoid  
124 contamination. Geochemical data was obtained at different tube voltage, 10 kV for Al, Si, S, Cl,  
125 K, Ca, Ti, Mn, Fe and 30 kV for Zn, Br, Sr, Rb, Zr (Richter et al., 2006).

126

127

### 128 3.3 Macro-fauna

129

130 To study mollusc shells, samples were taken every 2 cm and sieved at 1mm. Macro-fauna  
131 samples were taken at fixed volume (100  $\text{cm}^3$ ). Individuals were determined to the lower  
132 taxonomic level possible (species or genera) and counted. Assemblage structure was estimated by  
133 mean of species richness (S), taxon abundance ( $n_i$ ) and total abundance (N).

134

135 3.4 Geochronology

136  
137 The chronology of core MM2 was carried out using  $^{137}\text{Cs}$  and  $^{210}\text{Pb}$  method on a centennial time-  
138 scale by gamma spectrometry at the Géosciences Montpellier Laboratory (Montpellier, France).  
139  $^{14}\text{C}$  analyses were realized on mollusk shells at the Laboratoire de Mesure on ARTEMIS in CEA  
140 institute at Saclay. These measurements were obtained from monospecific samples of  
141 *Cerastoderma glaucum* at each level.  $^{14}\text{C}$  ages were corrected for reservoir age (see Sabatier et  
142 al., 2010 for method) and converted to calendar years using the computer program OxCal v4.2  
143 (Bronk Ramsey, 2001, 2008) at two standard deviations (see chapter 4.3).

144

145 3.5 Spectral analyses

146 Cyclic patterns in the Mar Menor lagoonal sequence were studied from spectral analyses by using  
147 two methods in order to reduce possible biases of a single method (Desprat et al., 2003). We used  
148 the maximum entropy method (MEM) and the multi-taper method (MTM). The MEM selects the  
149 spectrum with the highest entropy, which represents the least biased estimate for the given  
150 information, or put in other terms, the maximally noncommittal with regard to missing  
151 information (Harremoës and Topsoe, 2001). The spectrum obtained by this method shows an  
152 excellent frequency resolution with sharp spectral features (Berger et al., 1991; Dubar, 2006;  
153 Pardo-Iguzquiza and Rodriguez-Tovar, 2006). The MTM is a non-parametric method that (1)  
154 reduces the variance of spectral estimates by combining multiple orthogonal windows in the time  
155 domain before Fourier transforming, and (2) provides a narrowband F-test useful to assess the  
156 significance of periodic components (Thomson, 1982, 1990; Percival and Walden, 1993).

157

158

## 159 4. Results

160

### 161 4.1 Core description

162

163 Photo, X-ray images, X-ray fluorescence and high-resolution grain-size analysis for MM2  
164 indicate several thin, coarse-grained layers preserved within mud sediments. These coarse layers  
165 are constituted by a mixture of shell debris and siliciclastic sand and have basal boundaries easily  
166 identified from a change to coarser grain size and darker colour on X-ray images (Figure 2a).  
167 These coarser grain size layers indicate “energetic” events, relative to the background  
168 sedimentation (i.e mud facies) and are probably link to washover events (storm or tsunami).

169

### 170 4.2 Sediment source

171 The terrigenous fraction in Mar Menor lagoon is mainly controlled by terrestrial and marine  
172 inputs. The core (MM2) was collected at 800 m from the sandy barrier and more than 8,500 m  
173 from the different river mouths. On our study site, watercourses are the source of fine fraction  
174 dispersed in the lagoon and marine inputs are characterized by coarse sands. The lagoon barrier  
175 beach sand samples show unimodal distribution with a mean grain population ranging between  
176 160 and 653  $\mu\text{m}$ . The percentages of this grain population decrease from the sea to the lagoon in  
177 surface samples (Figure 2b). The evolution with depth of this population displays eight main  
178 changes in MM2 core revealed by the grey bands on Figure 3. The main peaks of coarse sands  
179 occur around 290, 255, 210, 170, 150, 60, 40 and 5 cm (Figure 3).



180 Major chemical elements using the ITRAX core scanner provide high-resolution  
181 palaeoenvironmental information in a variety of sedimentary environments. In the present study  
182 we chose the ratio Si/Al and Zr/Al that better discriminate between the two source areas, marine  
183 vs drainage basin (Dezileau et al., 2011, Sabatier et al., 2012; Raji et al., 2015). The high Zr/Al  
184 ratio value is probably explained by the presence of heavy minerals (like zircon) from marine  
185 sand and the high Si/Al ratio is due to Quartz minerals in marine sand. Si/Al and Zr/Al ratios  
186 have the same evolution with depth, especially in the first three meters of the sediment core  
187 (Figure 4, shaded bands).

188 A fundamental step in the core analysis is to establish criteria to correctly identify overwash  
189 layers. We systematically used grain size variation and geochemical signatures (i.e. Si/Al and  
190 Zr/Al ratios). As the background sedimentation shows a fine silt facies, we consider values higher  
191 than 20% of the 63 $\mu$ m fraction as outlining “high energy” events (Figure 3). Positive anomalies  
192 of the Si/Al and Zr/Al ratios above 12 and 2.5 respectively (Figure 4), indicate a higher relative  
193 contribution of marine sand. The marine origin of these “high energy” events was also  
194 highlighting through molluscs identification (*Bittium reticulatum* and *Rissoa ventricosa*) (see  
195 chapter 4.3, Figure 6).

196

#### 197 4.3. Faunal variations

198

199 Macro-fauna analyses are a good indicator of a lagoon palaeo-isolation state. While total  
200 abundance and relative abundance of individuals of the different species is a good indicator of  
201 environmental stress and lagoon productivity, species richness is a good indicator of marine  
202 influence because species develop in different ranges of salinity, temperature and oxygenation

203 and colonization of marine species into the lagoon environments depends of the isolation degree  
204 and connectivity between both systems (Pérez-Ruzafa and Marcos, 1992; Pérez-Ruzafa et al.,  
205 2005). Figure 5 shows the variation of the number of species and total abundance (number of  
206 individuals in 100 cm<sup>3</sup>) along the studied time series. Taxon richness ranges between 0, at depths  
207 higher than 365 cm, and 18 reached at a 260 cm depth. The impoverished depths, after the earlier  
208 azoic one, corresponds to 302-362 cm with a mean of 4.76 taxons, 72-78 cm with a mean of 5  
209 taxons and 30-36 cm with a mean of 5.7 taxons. The depths with highest species richness are  
210 from 192 to 266 cm and from 81 to 186 cm. These depths would correspond to a higher marine  
211 influence. Above 150 cm takes place a progressive impoverishment in the number of species  
212 reflecting a progressive isolation of the Mar Menor from the Mediterranean Sea, with punctual  
213 peacks in species richness, probably related to episodes of rupture of the sandbar (Figure 5). The  
214 total abundance confirm

215 The most frequent species, present in more than 50% of the samples, excluding the azoic depths,  
216 are *Corbula gibba* (Olivi, 1792) (92.4%), *Bittium reticulatum* (da Costa, 1778) (84.9%), *Tellina*  
217 *sp* (78.9%), *Pusillina* (=Rissoa) *lineolata* (Michaud, 1830) (78.2%), *Acanthocardia*  
218 *paucicostata* (G. B. Sowerby II, 1834) (77.3%), *Cerastoderma glaucum* (Bruguière, 1789)  
219 (71.4%), *Anthalis sp* (63.9%), *Abra sp* (74.8%), *Loripes lacteus* (Linnaeus, 1758) (61.3%) and  
220 *Philine aperta* (Linnaeus, 1767) (59.7%). Hydrobiidae *sp* appear in 47.9 % of the samples, but is  
221 restricted to the upper 150 cm, constituting 61.5% of the assemblage at 15 cm depth section. This  
222 specie is a typical lagoon inhabitant. *Conus ventricosus* (Gmelin, 1791) appears only in the  
223 13.5% of the samples, comprised between 162 and 293 cm depth, reaching dominance up to 7%  
224 of the assemblage, but characterizes typical marine conditions, reinforced with the presence of  
225 abundant seurchin spines.

226 Data of Figure 6 show a main change in mollusc population at around 150-130 cm characterized  
227 by an increase of the most typical lagoonal specie *Hydrobia acuta*, whereas the abundance of  
228 species with marine affinity like *Pusillina* (=Rissoa) *lineolata* and *Conus ventricosus* decrease  
229 (Figure 6). This main change in mollusc population also reveals a major palaeoenvironmental  
230 change around 150 cm, this faunal variation is probably due to a change in environmental context  
231 from a lagoonal environment, with a marine influence to a more isolated environment.

232

#### 233 4.4 Age model

234

235 The chronology of core MM2 has been established for the last 6,500 years BP using  $^{137}\text{Cs}$ ,  $^{210}\text{Pb}$   
236 and (AMS)  $^{14}\text{C}$  dates on monospecific shell samples, geochemical analysis of mining-  
237 contaminated lagoonal sediments and palaeomagnetism (Dezileau et al., in prep). Radiocarbon  
238 age of lagoonal and marine organisms is usually older than the atmospheric  $^{14}\text{C}$  age and has to be  
239 corrected by subtraction of the “reservoir age” (Siani et al., 2001; Reimer and McCormac 2002;  
240 Zoppi et al., 2001; Sabatier et al., 2010; Dezileau et al., 2015). We evaluated the modern  
241 reservoir  $^{14}\text{C}$  age by comparing an age derived from  $^{137}\text{Cs}$ ,  $^{210}\text{Pb}$  data and geochemical analysis of  
242 mining-contaminated lagoonal sediments with an AMS  $^{14}\text{C}$  age of a pre-bomb mollusc shell (see  
243 Sabatier et al., 2010 for method). The reservoir age (R(t)) with a value of  $1003 \pm 62$   $^{14}\text{C}$  yr is 600  
244 yr higher than the mean marine reservoir age (around 400 yr) and may be explained by an  
245 isolation of the lagoon from the Mediterranean Sea. This high reservoir age value is similar to  
246 other estimates in different Mediterranean lagoons (Zoppi et al., 2001; Sabatier et al., 2010).  
247  $^{14}\text{C}$  ages were also obtained on a series of Holocene mollusc shells sampled at different depths of  
248 the ~2-m-long core MM2 (Figure 7, Dezileau et al., in prep). Comparing palaeomagnetic ages

249 and  $^{14}\text{C}$  ages versus depth, we show that the reservoir age has changed in the past and was lower  
250 (505 yr) than the modern value (1003 yr, Dezileau et al., in prep). This change was also observed  
251 in another Mediterranean lagoons (Sabatier et al., 2010). In the Mar Menor lagoon, Linear  
252 Sedimentation Rate (LSR) obtained for the core MM2 suggest a low mean accumulation rate of  
253  $0.6 \text{ mm.yr}^{-1}$ , from the base to the top of the core.

254

## 255 5. Discussion

256

### 257 5.1 Site sensitivity to overwash deposits

258

259 Site sensitivity to overwash deposits may result from different factors such as barrier-elevation,  
260 sediment supply, inlet, and change in sea level (Donnelly and Webb, 2004; Scileppi and  
261 Donnelly, 2007, Dezileau et al., 2011). An increase of sea level induces a shift of the barrier  
262 landward. Therefore, an increase of sand layers in a sediment core may be due to a sea level  
263 change. In the Mediterranean Sea, the sea level has remained more or less constant during the last  
264 5000 yrs ( $< 2\text{m}$ , Pirazzoli, 1991; Lambeck and Bard, 2000). Before this period, a significant  
265 change in sea level occurred. During the first phase of lagoonal sediment deposit (between 6500  
266 and 5000 years Cal BP), the number of sand layers is low. The sandy barrier was probably at  
267 more than 1 km from the present position and may probably explain why sand layers are not  
268 observed. The strong increase in coarse grain layer frequency after ca 5400 years Cal BP can be  
269 explained by a migration of the barrier up to a position, which is not far away from the present  
270 position.

271 Fauna content reveals a major palaeoenvironmental change around 150 cm (i.e. 2400 yr cal BP,  
272 Figure 6). Such change is probably due to a shift from a leaky lagoon to a restricted and choked  
273 lagoon environment, sensu Kjerfve (1996). Thus, after this date (i.e 2400 yr cal BP) the barrier  
274 was continuous with sometimes inlet formation in relation to intense overwash events. To  
275 conclude, between 2400 yr cal BP and today, the lagoon is isolated from the sea. During this  
276 period the general morphology of the lagoon and the barrier have not changed drastically.  
277 Between 5400 yr cal BP and 2400 yr cal BP the lagoon was less isolated from the Mediterranean  
278 Sea, typical from a leaky lagoon environment. During this period, fine sediments were  
279 accumulated. The lagoon experienced quiescent sedimentation probably protected behind a sandy  
280 barrier more or less continuous. The presence of sand layers may be interpreted by intense  
281 overwash events. Between 6500-5400 yrs BP, the morphology of the lagoon and the barrier is  
282 different. The position of the sandy barrier was far away from the present position. In that case,  
283 the number and the intensity of surge events recorded are not comparable to the upper part of the  
284 core (Figures 3 and 8). During this period, the lack of sand layers does not mean no surge events  
285 but simply they are not recorded.

286

## 287 5. 2 Storms or tsunamis?

288 The Zr/Al and Si/Al ratios of sandy layers are above 12 and 2.5 respectively (Figure 8),  
289 indicating a higher relative contribution of marine sand. The marine origin of these “high energy”  
290 events was also highlighted through molluscs identification (*Bittium reticulatum* and *Rissoa*  
291 *ventricosa*, Figure 8). This multiproxy approach suggests the occurrence of eight periods of  
292 increase of overwash events reflecting perturbations of coastal hydrodynamic due to palaeostorm  
293 or palaeotsunami events (grey band on Figure 8).

294 Both tsunamis and storms induce coastal flooding. It is difficult to discriminate storm and  
295 tsunami deposits (Kortekaas and Dawson, 2007; Morton et al., 2007; Engel and Brückner, 2011).  
296 The coarse-grained layers observed in the core MM2 could be a signature of tsunamis or storms.  
297 Records of historic and contemporary coastal hazards (storms and tsunamis) may help us to  
298 determine which historical events left a sedimentological signature in the Mar Menor lagoon.  
299 In textual archives, extreme storm events were described due to the strong economic and societal  
300 impact of these events (Seisdedos et al., 2013). For the last 200 years, 27 storms affected the  
301 coast of Murcia. Among all of these storms, some seems to be more catastrophic. The storm of  
302 November first, 1869 produced the wreckage of a numerous ships in the Torrevieja harbour.  
303 Between Isla Grosa and San Pedro del Pinatar more than thirty-five ships sank and crashed. In  
304 the Mar Menor lagoon, fifty fishing boats were destroyed and thrown to the ground. Wave  
305 heights associated with this storm were estimated higher than 8 m off the La Manga sandbar.  
306 This severe storm also affected La Union and Cartagena cities destroying houses and paralyzing  
307 it for many days. From the hydrological and ecological point of view, the 1869 storm led to  
308 drastic and persistent changes in the salinity of the lagoon and to the colonization of new species  
309 of marine origin (Navarro, 1927), affecting also the fisheries in the lagoon (Pérez-Ruzafa et al.,  
310 1991). There are historical references to some other storms that led to the breaking of the sandbar  
311 in the Mar Menor (in 1526, 1676, 1687, 1690, 1692, 1694, 1706, 1762, 1765, 1787, 1795)  
312 (Jiménez de Gregorio, 1957; Pérez-Ruzafa et al., 1987), although there is no information about  
313 their magnitude, the extent and exact location of the breaks and their impact on the lagoon  
314 environment. Some ups and downs in the number of species observed in Figure 5 could be  
315 related to these events, but an extensive and detailed study would be required for understanding

316 the relationship between the frequency, duration and intensity of the storms and the spatial and  
317 temporal scales of their effects and their impact on the fossil record.

318 Different tsunamis occurred on the Spanish coasts, they are more catastrophic and intense on the  
319 Atlantic than on the Mediterranean side (Alvarez-Gomez et al., 2011). In the occidental part of  
320 the Mediterranean area, there are historical disastrous tsunami events recorded. In Northern  
321 Algeria, in addition to the 2003 tsunami, the first well documented event remains the tsunami in  
322 the Djijelli Area associated with the seismic event of August 1856, which was also recorded in  
323 the Balearic Islands (Maouche et al., 2009). In the Alboran Sea area some reports mention  
324 tsunamis that affected the African and Spanish coasts in 1790, 1804 and 1522 (IGN, 2009). For  
325 an earthquake magnitude 6.8 (2003 Boumerdes earthquake) with its epicenter calculated at 15 km  
326 offshore of Zemmouri, Wang and Liu (2005) show a regional character of the tsunami  
327 phenomenon from a numerical simulation. The tsunami propagating from the Algerian coast to  
328 the Murcia Province has a lesser amplitude and the tsunami wave height is low ( $< 25$  cm). The  
329 Boumerdes-Zemmouri tsunami did not induce any damage along the province of Murcia and the  
330 La Manga sandbar. Alvarez-Gomez et al. (2011) identified the hazardous sources and the areas  
331 where the impact of tsunamis is greater from numerical simulations. From a set of 22 seismic  
332 tsunamigenic sources, the Maximum Wave Elevation was estimated between 0.5 and 1 m along  
333 the South-Eastern Spanish coast. All these historical events have been classified as a magnitude  
334 between 1 and 3 in the Tsunami Intensity Scale (on a scale of 6 for a maximum intensity,  
335 Maramai et al., 2014). Since these different historical events have a magnitude equal or lower  
336 than the Boumerdes-Zemmouri tsunami (3 in the Tsunami Intensity Scale), and that this event did  
337 not affect significantly La Manga sandbar and the Province of Murcia, considering the available  
338 data, historical tsunami events do not seem to be associated to the different sand layers in the

339 Mar Menor lagoon for the last 500 years. From the “Catálogo de Tsunamis en las Costas  
340 Españolas”, no tsunamis are recorded along the South Eastern coast of Spain from -218 BC to  
341 1756 AD. No information on the existence of tsunamis is recorded over longer periods of time.  
342 However, more than 100 boulders were identified along the coastal zone of Algiers and Maouche  
343 et al. (2009) suggested that the deposition of the biggest boulders could be attributed to tsunami  
344 events. The radiocarbon results highlight two groups of boulders dated to around 419 AD and  
345 1700 AD. Although no historical accounts report these events, tsunami events are extremely rare  
346 and mainly of low magnitude and cannot be at the origin of the different sand layers in the Mar  
347 Menor lagoon.

348 To determine which historical events may let sandy layers, we compared our high-resolution  
349 record of past extreme sea events from the core MM2 to the catalogue of historical storm and  
350 tsunami events in the area. The first coarse-grained event layer has been dated at 80 cal. BP (i.e.  
351 1880 A.D+/-30 years). This sandy deposit could be associated to the storm of November first,  
352 1869, recorded in many city archives between Cartagena and Torre Vieja and in the Mar Menor,  
353 and considered as the most catastrophic storm event in the Province of Murcia for the last 200  
354 years. In the core MM2, no sand layers are consistent with the Algerian tsunamis dated to around  
355 419 AD and 1700 AD (Figure 8). There is evidence that this sand layer is compatible with large  
356 storm waves.

357

### 358 5.3 Storm activity in the context of past climatic changes

359

360 Based on our  $^{14}\text{C}$  age model, marine coarse grained event layers occurred around 5250, 4000,  
361 3600, 3010, 2300, 1350, 650 and 80 years cal BP. Except one period dated at 3600 years cal BP,



362 the seven other periods of most frequent surge events in the Mar Menor lagoon seem to coincide  
363 with the coldest periods in Europe during the late Holocene, taking into account chronological  
364 uncertainty (Figure 8, Bond et al., 2001). A spectral analysis was performed on the ca 6.5-kyr  
365 time series of the sand percentage from the MM2 sequence. The results show four major  
366 frequencies with high spectral power densities and significant F-test values at ca  $8 \times 10^{-4}$ ,  $1.4 \times 10^{-3}$ ,  
367  $1.8 \times 10^{-3}$ , and  $3.1 \times 10^{-3} \text{ yr}^{-1}$  (Figure 9A). Considering the full width at half maximum (FWHM) of  
368 these peaks on the MTM spectrum, this yields respective periodicities of  $1228 \pm 327$ ,  $732 \pm 80$ ,  
369  $562 \pm 58$ , and  $319 \pm 16 \text{ yr}$  for the MM2 sand % proxy. Multi-centennial to millennial timescale  
370 climate variabilities similar to these periodicities have been reported in the literature for the  
371 Holocene (Bond et al., 1997, 2001; Langdon et al., 2003; Debret et al., 2007, 2009; Wanner et al.,  
372 2011; Kravchinsky et al., 2013; Soon et al., 2014). Amongst the well-known proxies that have  
373 revealed a millennial-scale climate variability during the Holocene, the ice-rafted debris (IRD)  
374 indices in North Atlantic developed by Bond et al. (1997, 2001) present a cyclicity of  $1470 \pm 500$   
375 yr, which matches the  $1228 \pm 327 \text{ yr}$  periodicity evidenced in the Mar Menor lagoon, considering  
376 the respective uncertainties on the periodicities. When filtering the raw data of the Mar Menor  
377 sand % record by a Gaussian filter with a frequency of  $8 \times 10^{-4} \text{ yr}^{-1}$  (1228 years), six cycles appear  
378 with a noteworthy enhancement of the cyclic amplitude after 5500 cal yr BP (Figure 9B). The  
379 five ascending phases occurring on the 1228-yr filtered curve at ca 5715/5115, 4525/3945,  
380 3365/2775, 2145/1215, and 575/-35 cal yr BP approximate the high storm activity periods  
381 evidenced in the French Mediterranean lagoon of Pierre-Blanche for the last 7000 years (Sabatier  
382 et al., 2012).

383 The origin of the storminess periods evidenced by the spectral analysis in the Mar Menor lagoon  
384 can be discussed in the light of previous works mentioning analogous climate variabilities during  
385 the Holocene. Bond et al. (1997, 2001) associated the  $1470 \pm 500 \text{ yr}$  IRD cycle to a solar forcing,

386 amplified by a change of North Atlantic Deep Water production. Langdon et al. (2003) found a  
387 sub-millennial climate oscillation in Scotland possibly related to the North Atlantic thermohaline  
388 circulation (THC). Moreover, Debret et al. (2007, 2009) showed a cyclicity of 1500 yr since the  
389 Mid-Holocene probably link to an internal forcing due to the THC.

390 Concerning the multi-centennial periodicities, Soon et al. (2014) used global proxies to evidence  
391 a 500-yr fundamental solar mode and to identify intermediate derived cycles at 700 and 300-yr  
392 which could be rectified responses of the Atlantic THC to external solar modulation and pacing.  
393 Kravchinsky et al. (2013) found also a 500-yr climate cycle in the southern Siberia presumed to  
394 be derived by increased solar insolation and possibly amplified by other mechanisms. Some  
395 authors found a relationship between the ca 700-yr period and the monsoonal/ITCZ regimes in  
396 equatorial Africa (Russell et al., 2003; Russell and Johnson, 2005), southern Asian (Staubwasser  
397 et al., 2003), and eastern Arabian Sea (Sarkar et al., 2000), while other authors suggested that the  
398 ca 700-800 yr period could be a subharmonic mode derived from the fundamental 1500-year  
399 cycle of the THC (Von Rad et al., 1999; Wang et al., 1999). Besides, Rimbu et al. (2004)  
400 mentioned a 700 yr variability from sea-surface temperature (SST) records in the tropical and  
401 North Atlantic. Hence, our results seem to indicate that the Late Holocene multi-centennial  
402 variability of the cyclogenesis in Western Mediterranean was steered by both, external (solar) and  
403 internal (THC/ITCZ) forcings. Further investigations of additional sequences and high-resolution  
404 coastal imagery will be required to assert reliably the origin of these multi-centennial periods in  
405 the Mediterranean area.

406

## 407 7. Conclusion

408 This study provides a 6500-yr high-resolution record of past overwash events using a multi-proxy

409 approach of a sediment core from the Mar Menor lagoon in Spain in the Western Mediterranean  
410 Sea. Eight sandy layers are preserved in the core and seems to be associated to periods of  
411 increased extreme sea events. The results indicate little likelihood of a tsunami origin for these  
412 coarse grained layers, although historical tsunami events are recorded in this area. These surge  
413 events seem to coincide with climatic cold periods in Europe during the late Holocene,  
414 suggesting a control by a climatic mechanism for periods of increased storm activity. From the  
415 available data, we have identified seven periods of high storm activity at around 5250, 4000,  
416 3600, 3010, 2300, 1350, 650 and 80 years cal BP. Except one period dated at 3600 years cal BP,  
417 the seven other periods of most frequent surge events in the Mar Menor lagoon seem to coincide  
418 with the coldest periods in Europe during the late Holocene, taking into account chronological  
419 uncertainty. Spectral analyses performed on the sand % revealed four major periodicities of 1228  
420  $\pm 327$ , 732  $\pm 80$ , 562  $\pm 58$ , and 319 $\pm 16$  yr. The origin of the storminess periods evidenced by the  
421 spectral analysis in the Mar Menor lagoon can be discussed in the light of previous works  
422 mentioning analogous climate variabilities during the Holocene. Our results seem to indicate that  
423 the Late Holocene multi-centennial variability of the cyclogenesis in Western Mediterranean was  
424 steered by both, external (solar) and internal (THC/ITCZ) forcings. However, further  
425 investigations, such as additional coring, high-resolution coastal imagery, are needed to better  
426 constrain the main cause of these multiple-events.

427

428

429 Acknowledgments

430

431 The authors would like to thank all participants in the coring expedition, particularly E. Regnier  
432 (Technician, LSCE - IPSL, Paris) for his collaboration in the various stages of this study. This  
433 study is funded by the MISTRALS PALEOMEX project. We thank the Laboratoire de Mesure  
434  $^{14}\text{C}$  (LMC14) ARTEMIS in the CEA Institute at Saclay (French Atomic Energy Commission) for  
435 the  $^{14}\text{C}$  analyses. This article benefited through constructive reviews by Stella Kortekaas and  
436 Suzanne Leroy.

437

438

## 439 References

440

441 Álvarez-Gómez, J. A., González, M., and Otero, L.: Tsunami hazard at the Western  
442 Mediterranean Spanish coast from seismic sources, *Natural Hazards and Earth System*  
443 *Science*, 11, 227-240, 2011.

444 Berger, A., Melice, J.-L., Hinnov, L.: A strategy for frequency spectra of Quaternary climate  
445 records. *Climate Dynamics* 5, 227-240, 1991.

446 Bond, G., Kromer, B., Beer, J., Muscheler, R., Evans, M. N., Showers, W., Hoffmann, S., Lotti-  
447 Bond, R., Hajdas, I., and Bonani, G.: Persistent solar influence on North Atlantic climate  
448 during the Holocene, *Science*, 294, 2130-2136, 2001.

449 Bond, G., Showers, W., Cheseby, M., Lotti, R., Almasi, P., DeMenocal, P., Priore, P., Cullen, H.,  
450 Hajdas, I., Bonani, G.: A pervasive millennial-scale cycle in North Atlantic Holocene and  
451 Glacial climates. *Science* 278, 1257-1266, 1997.

452 Bronk Ramsey, C., Development of the Radiocarbon calibration program OxCal, *Radiocarbon*,  
453 43, 355-363, Proceedings of 17th International  $^{14}\text{C}$  Conference, 2001.

454 Bronk Ramsey, C., Deposition models for chronological records, *Quaternary Science reviews*,  
455 27, 42-60, 2008.

456 Debret, M., Bout-Roumazeilles, V., Grousset, F., Desmet, M., McManus, J.F., Massei, N., Sebag,  
457 D., Petit, J.-R., Copard, Y., Trentesaux, A.: The origin of the 1500-year climate cycles in  
458 Holocene North-Atlantic records. *Climate of the Past* 3, 569-575, 2007.

459 Debret, M., Sebag, D., Crosta, X., Massei, N., Petit, J.-R., Chapron, E., Bout-Roumazeilles, V.:  
460 Evidence from wavelet analysis for a mid-Holocene transition in global climate forcing.  
461 *Quaternary Science Reviews* 28, 2675-2688, 2009.

462 Desprat, S., Sanchez-Goni, M.F., Loutre, M.-F.: Revealing climatic variability of the last three  
463 millennia in northwestern Iberia using pollen influx data. *Earth and Planetary Science*  
464 *Letters* 213, 63-78, 2003.

465 Dezileau, L., Pérez-Ruzafa, A., Camps P., Blanchemanche P., Grafenstein U., Holocene  
466 variations of radiocarbon reservoir ages in the Mar Menor lagoon system, *Radiocarbon*, in  
467 prep.

468 Dezileau, L., Sabatier, P., Blanchemanche, P., Joly, B., Swingedouw, D., Cassou, C., Castaings,  
469 J., Martinez, P., and Von Grafenstein, U.: Intense storm activity during the Little Ice Age  
470 on the French Mediterranean coast, *Palaeogeography, Palaeoclimatology, Palaeoecology*,  
471 299, 289-297, 2011.

472 Dezileau L., Lehu R., Lallemand S., Hsu S-K., Babonneau N., Ratzov G., Lin A.T., Dominguez  
473 S., Historical reconstruction of submarine earthquakes using <sup>210</sup>Pb, <sup>137</sup>Cs and <sup>241</sup>Am  
474 turbidite chronology and radiocarbon reservoir age estimation off East Taiwan.  
475 *Radiocarbon*. doi:10.1017/RDC.2015.3, 2016.

476 Donnelly, J. P., Webb III, T., Murnane, R., and Liu, K.: Backbarrier sedimentary records of  
477 intense hurricane landfalls in the northeastern United States, *Hurricanes and Typhoons:*  
478 *Past, Present, and Future*, 58-95, 2004.

479 Dubar, M.: Approche climatique de la période romaine dans l'est du Var : recherche et analyse  
480 des composantes périodiques sur un concrétionnement centennal (Ier-IIe siècle apr. J.-C.)  
481 de l'aqueduc de Fréjus. *ArchéoSciences* 30, 163-171, 2006.

482 Engel, M., and Brückner, H.: The identification of palaeo-tsunami deposits—a major challenge in  
483 coastal sedimentary research, *Dynamische Küsten—Grundlagen, Zusammenhänge und*  
484 *Auswirkungen im Spiegel angewandter Küstenforschung. Proceedings of the 28th Annual*  
485 *Meeting of the German Working Group on Geography of Oceans and Coasts*, 2011, 22-25,

486 Gaertner, M.A., Jacob, D., Gil, V., Domínguez, M., Padorno, E., Sánchez, E., Castro, M. :  
487 Tropical cyclones over the Mediterranean Sea in climate change simulations. *Geophysical*  
488 *Research Letters* 34. doi:10.1029/2007GL029977, 1-5, 2007.

489 Harremoës, P., Topsoe, F.: Maximum entropy fundamentals. *Entropy* 3, 191-226, 2001.

490 IGN: Catalogo de Tsunamis en las Costas Espanolas. Instituto Geografico Nacional, [www.ign.es](http://www.ign.es),  
491 2009.

492 Jimenez de Gregorio, F.: *El Municipio de San Javier en la historia del Mar Menor y su ribera.*  
493 Ayuntamiento de San Javier, Murcia, 1957.

494 Kelletat, D., and Schellmann, G.: Tsunamis on Cyprus: field evidences and 14C dating results,  
495 *Zeitschrift für Geomorphologie*, NF, 19-34, 2002.

496 Kjerfve, B.: Coastal lagoons. In Kjerfve B (ed). *Coastal lagoon processes*. Elsevier  
497 Oceanography Series 60: 1-8, 1994.

498 Kortekaas, S., and Dawson, A.: Distinguishing tsunami and storm deposits: an example from  
499 Martinhal, SW Portugal, *Sedimentary Geology*, 200, 208-221, 2007.

500 Kravchinsky, V.A., Langereis, C.G., Walker, S.D., Dlusskiy, K.G., White, D.: Discovery of  
501 Holocene millennial climate cycles in the Asian continental interior: Has the sun been  
502 governing the continental climate? *Global and Planetary Change* 110, 386-396, 2013.

503 Lambeck, K., and Bard, E.: Sea-level change along the French Mediterranean coast for the past  
504 30 000 years, *Earth and Planetary Science Letters*, 175, 203-222, 2000.

505 Langdon, P.G., Barber, K.E., Hugues, P.D.M.: A 7500-year peat-based palaeoclimatic  
506 reconstruction and evidence for an 1100-year cyclicity in bog surface wetness from Temple  
507 Hill Moss, Pentland Hills, southeast Scotland. *Quaternary Science Reviews* 22, 259-274,  
508 2003.

509 Lionello, P., Bhend, J., Buzzi, A., Della-Marta, P.M., Krichak, S., Jansá, A., Maheras, P., Sanna,  
510 A., Trigo, I.F., Trigo, R. : Cyclones in the Mediterranean region: climatology and effects on  
511 the environment, in *Mediterranean Climate Variability*. In: Lionello, P., Malanotte-Rizzoli,  
512 P., Boscolo, R. (Eds.), *Mediterranean Climate Variability. : Developments in Earth and*  
513 *Environmental Sciences*, 4. Elseviered., 324–372, 2006.

514 Maouche, S., Morhange, C., and Meghraoui, M.: Large boulder accumulation on the Algerian  
515 coast evidence tsunami events in the western Mediterranean, *Marine Geology*, 262, 96-104,  
516 2009.

517 Maramai, A., Brizuela, B., and Graziani, L.: The Euro-Mediterranean Tsunami Catalogue,  
518 *Annals of Geophysics*, 57, S0435, 2014.

519 Morhange, C., Marriner, N., and Pirazzoli, P. A.: Evidence of Late-Holocene Tsunami Events in  
520 Lebanon *Z. Geomorphol NFSuppl.-Bd.*, 146, 81-95, 2006.

521 Morton, R. A., Gelfenbaum, G., and Jaffe, B. E.: Physical criteria for distinguishing sandy  
522 tsunami and storm deposits using modern examples, *Sedimentary Geology*, 200, 184-207,  
523 2007.

524 Navarro, F.: Observaciones sobre el Mar Menor (Murcia). Notas y resúmenes del Instituto  
525 Español de Oceanografía, Ser. II, 16:1-63, 1927.

526 Paillard, D., Labeyrie, L., Yiou, P.: Macintosh program performs time-series analysis. *EOS*  
527 *Transactions AGU* 77(39), 379-379, 1996.

528 Pardo-Iguzquiza, E., Rodriguez-Tovar, F.J.: Maximum entropy spectral analysis of climatic time  
529 series revisited: Assessing the statistical significance of estimated spectral peaks. *Journal of*  
530 *Geophysical Research* 111, D10102, 2006.

531 Percival, D.B., Walden, A.T.: *Spectral analysis for physical applications: multitaper and*  
532 *conventional univariate techniques*. Cambridge University Press, New York, 583 p, 1993.

533 Pérez-Ruzafa, A., Marcos, C., Pérez-Ruzafa, I., and Ros, J.: Evolución de las características  
534 ambientales y de los poblamientos del Mar Menor (Murcia, SE de España), *Anales de*  
535 *Biología*, 1987, 53-65,

536 Pérez-Ruzafa, A., Marcos-Diego, C., and Ros, J.: Environmental and biological changes related  
537 to recent human activities in the Mar Menor (SE of Spain), *Marine Pollution Bulletin*, 23,  
538 747-751, 1991.

539 Pérez-Ruzafa, A., Marcos-Diego, C.: Colonization rates and dispersal as essential parameters in  
540 the confinement theory to explain the structure and horizontal zonation of lagoon benthic  
541 assemblages. *Rapp. Comm. int. Mer Médit.* 33: 100, 1992.

542



543 Pérez-Ruzafa, A., Marcos, C., and Gilabert, J.: The ecology of the Mar Menor coastal lagoon: a  
544 fast-changing ecosystem under human pressure, *Coastal Lagoons*. CRC Press, Boca Racon,  
545 392-421, 2005.

546 Pirazzoli, P. A.: World atlas of Holocene sea-level changes, *Elsevier Oceanography Series*, 58, 1-  
547 280, 1991.

548 Raji, O., Dezileau L., Snoussi M., and Niazi, S.: Extreme sea events during the last millennium in  
549 North-East of Morocco. *Natural Hazards and Earth System Sciences*, 15,203-211, 2015.

550 Reimer P.J., McCormac F.G.: Marine radiocarbon reservoir corrections for the Mediterranean  
551 and Aegean seas. *Radiocarbon* 44(1):159–66, 2002.

552 Rimbu, N., Lohmann, G., Lorenz, S.J., Kim, J.H., Schneider, R.R.: Holocene climate variability  
553 as derived from alkenone sea surface temperature and coupled ocean-atmosphere model  
554 experiments. *Climate Dynamics* 23, 215-227, 2004.

555 Russell, J.M., Johnson, T.C.: Late Holocene climate change in the North Atlantic and equatorial  
556 Africa: Millennial-scale ITCZ migration. *Geophysical Research Letters* 32, L17705, 2005.

557 Russell, J.M., Johnson, T.C., Talbot, M.R.: A 725 yr cycle in the climate of central Africa during  
558 the late Holocene. *Geology* 31(8), 677-680, 2003.

559 Sabatier, P., Dezileau, L., Blanchemanche, P., Siani, J., Condomines, M., Bentaleb, I., Piques, G.:  
560 Holocene variations of radiocarbon reservoir ages in a Mediterranean lagoonal system.  
561 *Radiocarbon*, 52, (1), 91-102, 2010.

562 Sabatier, P., Dezileau, L., Colin, C., Briquieu, L., Bouchette, F., Martinez, P., Siani, G., Raynal,  
563 O., Von Grafenstein, U.: 7000 years of paleostorm activity in the NW Mediterranean Sea in  
564 response to Holocene climate events. *Quaternary Research* 2012, 1-11, 2012.

565 Sarkar, A., Ramesh, R., Somayajulu, B.L.K., Agnihotri, R., Jull, A.J.T., Burr, G.S.: High  
566 resolution Holocene monsoon record from the eastern Arabian Sea. *Earth and Planetary*  
567 *Science Letters* 177, 209-218, 2000.

568 Scileppi, E., Donnelly, J.P. : Sedimentary evidence of hurricane strikes in western Long Island,  
569 NY. *Geochemistry, Geophysics and Geosystems* 8, Q06011. doi:10.1029/ 2006GC001463,  
570 2007.

571 Seisdedos, J., Mulas, J., González de Vallejo, L. I., Rodríguez Franco, J. A., Gracia, F. J., Del  
572 Río, L., y Garrote, J. :Estudio y cartografía de los peligros naturales costeros de la región  
573 de Murcia. *Boletín Geológico y Minero*, 124 (3): 505-520, 2013.

574 Siani G., Paternò M., Michel E., Sulpizio R., Sbrana A., Arnold M., Haddad G. : Mediterranean  
575 sea surface radiocarbon age changes since the last glacial maximum. *Science*  
576 294(5548):1917–20, 2001.

577 Soon, W., Velasco Herrera, V.M., Selvaraj, K., Traversi, R., Usoskin, I., Arthur Chen, C.-T.,  
578 Lou, J.-Y., Kao, S.-J., Carter, R.M., Pipin, V., Severi, M., Becagli, S.: A review of  
579 Holocene solar-linked climatic variation on centennial to millennial timescales: Physical  
580 processes, interpretative frameworks and a new multiple cross-wavelet transform  
581 algorithm. *Earth-Science Reviews* 134, 1-15, 2014.

582 Staubwasser, M., Sirocko, F., Grootes, P.M., Segl, M.: Climate change at the 4.2 ka BP  
583 termination of the Indus valley civilization and Holocene south Asian monsoon variability.  
584 *Geophysical Research Letters* 30(8), 1425, 2003.

585 Thomson, D.J.: Spectrum estimation and harmonic analysis. *Proceedings of the IEEE* 70(9),  
586 1055-1096, 1982.

587 Thomson, D.J.: Time series analysis of Holocene climate data. *Philosophical Transactions of the*  
588 *Royal Society of London, Series A, Mathematical and Physical Sciences* 330, 601-616,  
589 1990.

590 Trigo, I.F., Davies, T.D., Bigg, G.R., : Decline in Mediterranean rainfall caused by weakening of  
591 Mediterranean cyclones. *Geophysical Research Letters* 27, 2913–2916, 2000.

592 Von Rad, U., Schaaf, M., Michels, K.H., Schulz, H., Berger, W.H., Sirocko, F. A 5000-yr Record  
593 of Climate Change in Varved Sediments from the Oxygen Minimum Zone off Pakistan,  
594 Northeastern Arabian Sea. *Quaternary Research* 51, 39-53, 1999.

595 Wang, L., Sarnthein, M., Erlenkeuser, H., Grimalt, J., Grootes, P., Heilig, S., Ivanova, E.,  
596 Kienast, M., Pelejero, C., Pflaumann, U.: East Asian monsoon climate during the Late  
597 Pleistocene: high-resolution sediment records from the South China Sea. *Marine Geology*  
598 156, 245-284, 1999.

599 Wang, X., Liu, P.L.-F., : A numerical investigation of Boumerdes-Zemmouri (Algeria)  
600 earthquake and tsunami. *Computer Modeling in Engineering Science* 10 (2), 171–184,  
601 2005.

602 Wanner, H., Solomina, O., Grosjean, M., Ritz, S.P., Jetel, M.: Structure and origin of Holocene  
603 cold events. *Quaternary Science Reviews* 30, 3109-3123, 2011.

604 Zoppi U., Albani A., Ammerman A.J., Hua Q., Lawson E.M., Serandrei Barbero R. :Preliminary  
605 estimate of the reservoir age in the Lagoon of Venice. *Radiocarbon* 43(2A):489–94, 2001.

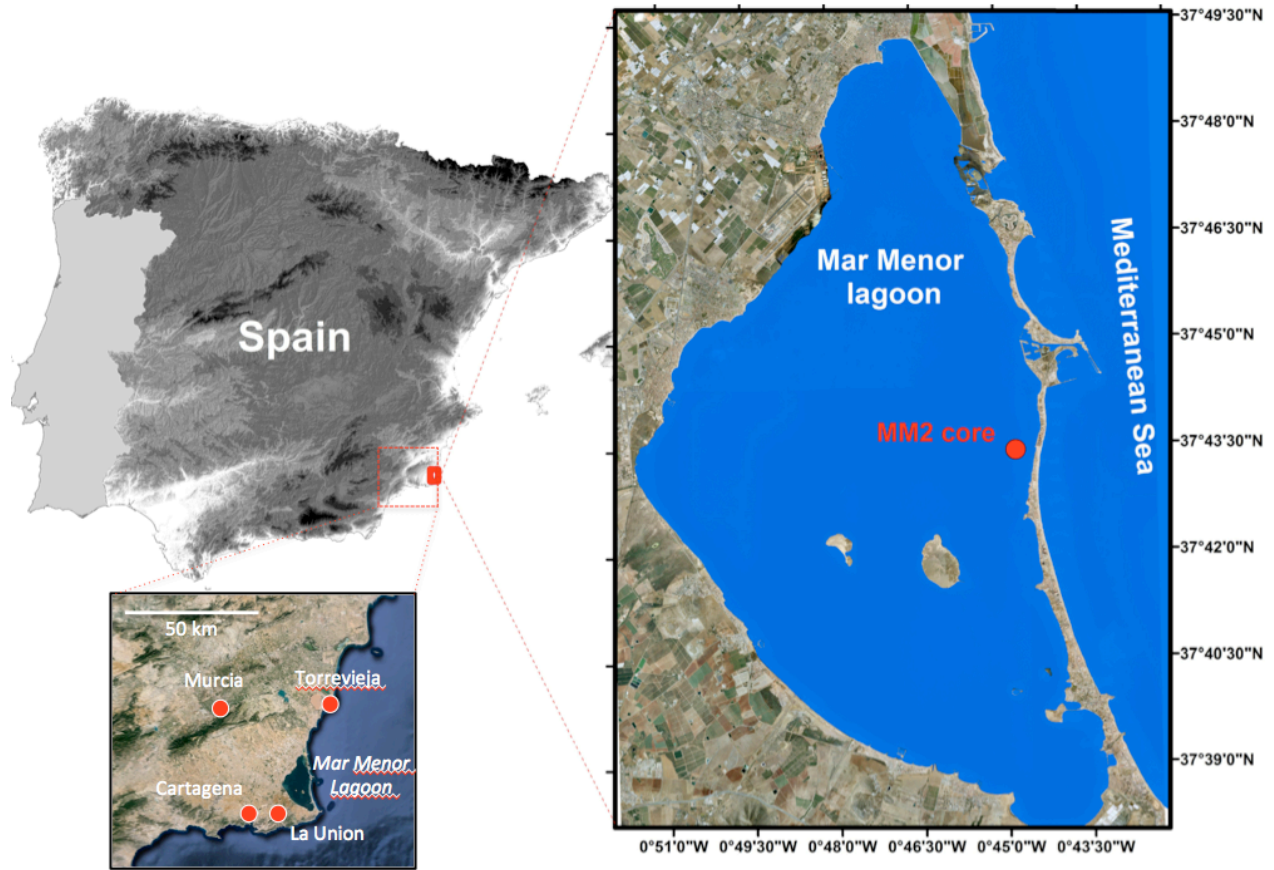
606

607

608

609 *Figures captions*

610  
611  
612  
613  
614  
615  
616  
617

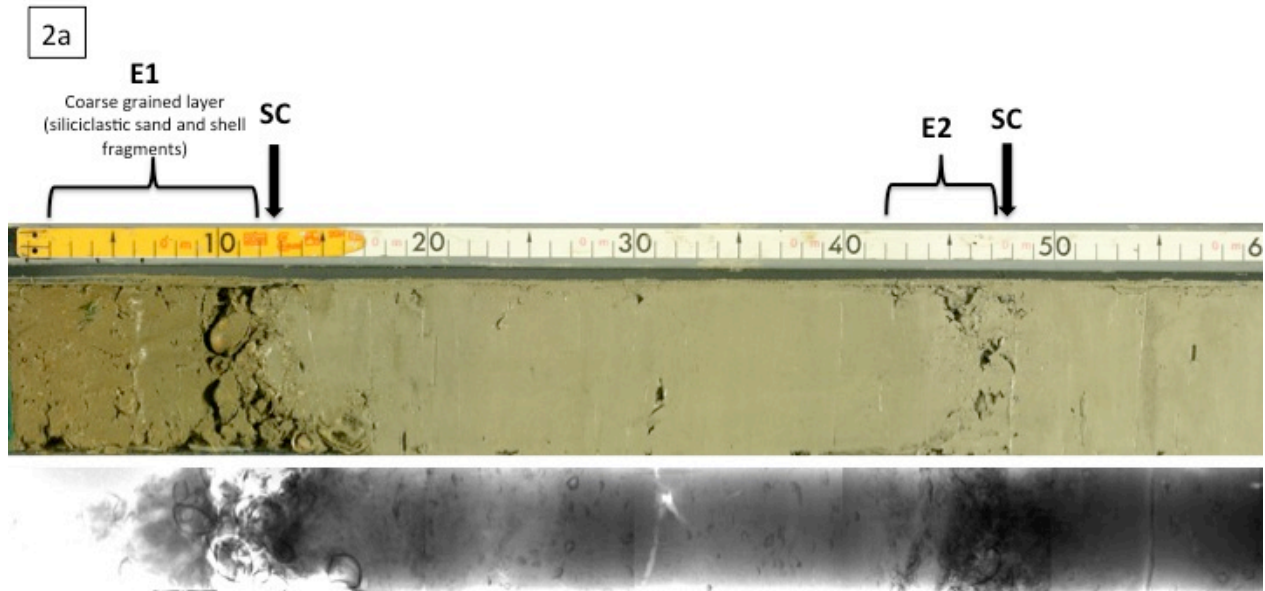


618  
619  
620  
621  
622  
623  
624  
  
625  
626  
627

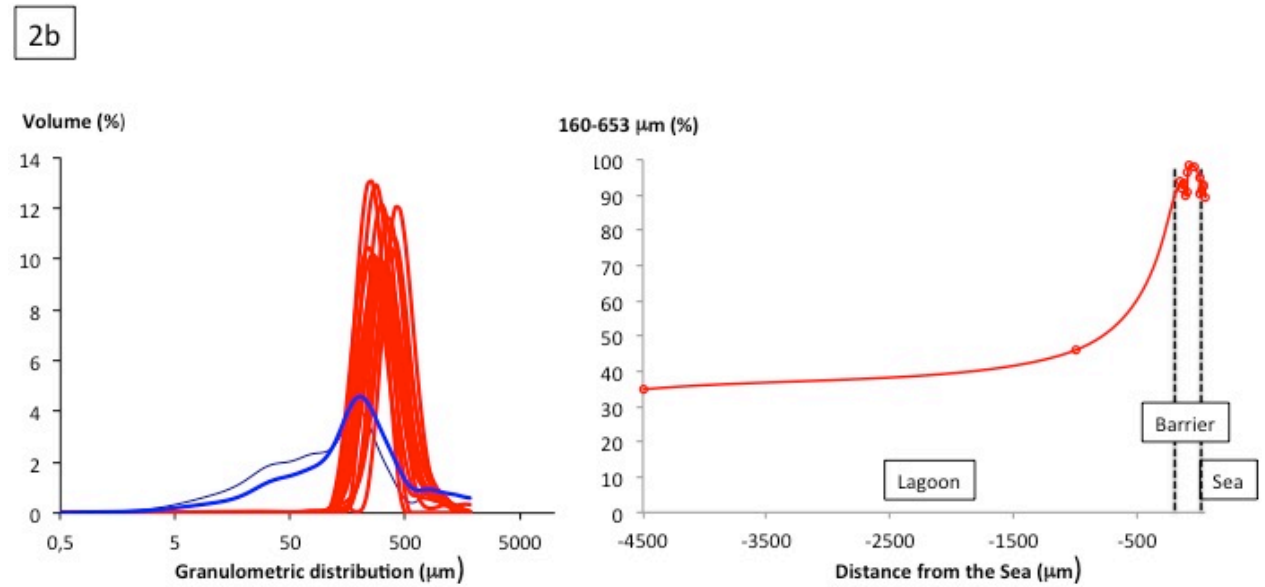
**Figure 1.** Map of the Mar Menor lagoon with localisation of the core MM2.

628

629



630



631

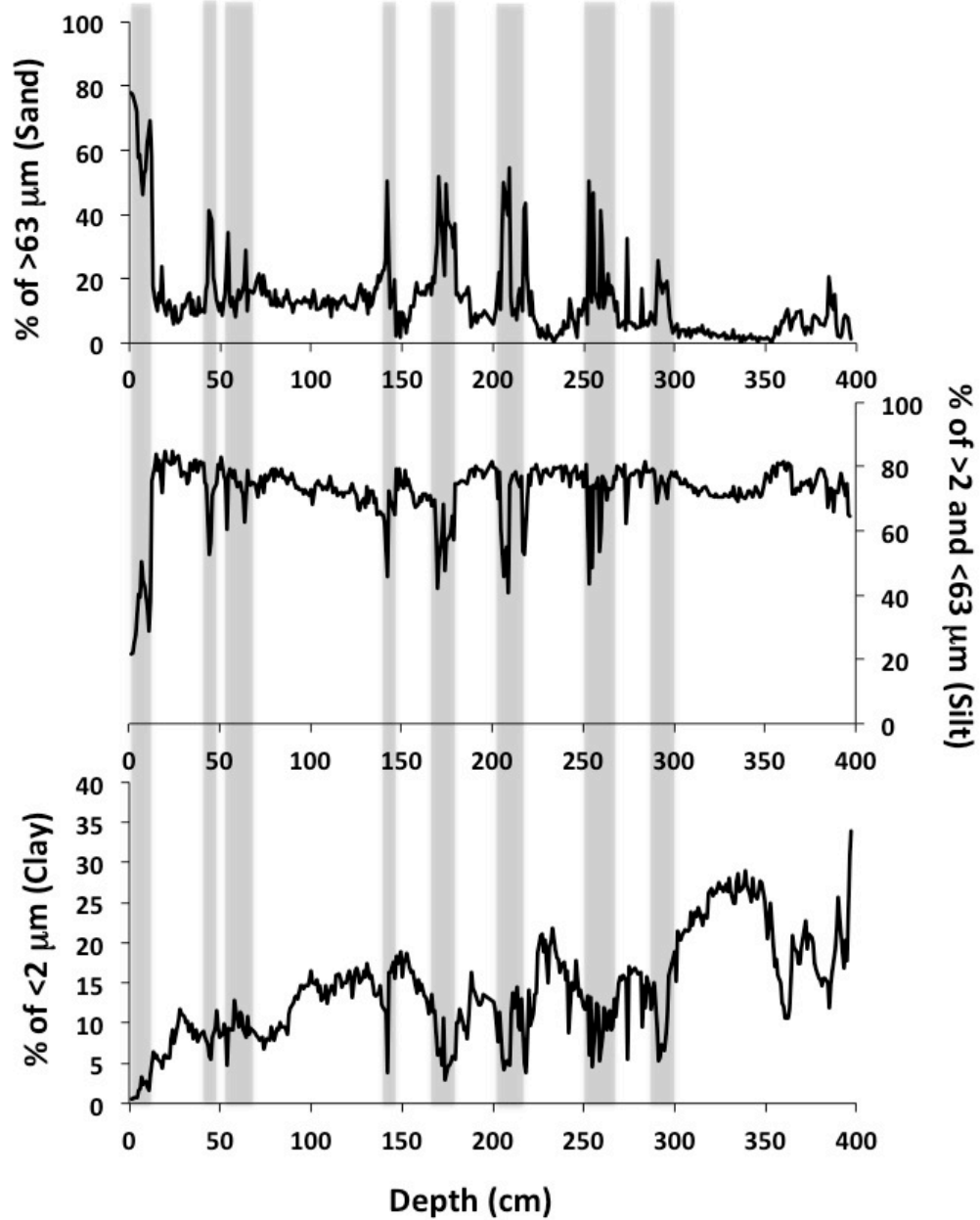
632

633 **Figure 2. a)** Photography and X-ray of the core MM2 (0 and 60 cm). Coarse grained layers are a

634 mixture of siliciclastic sand and shell fragments. These layers have often sharp contacts (SC)

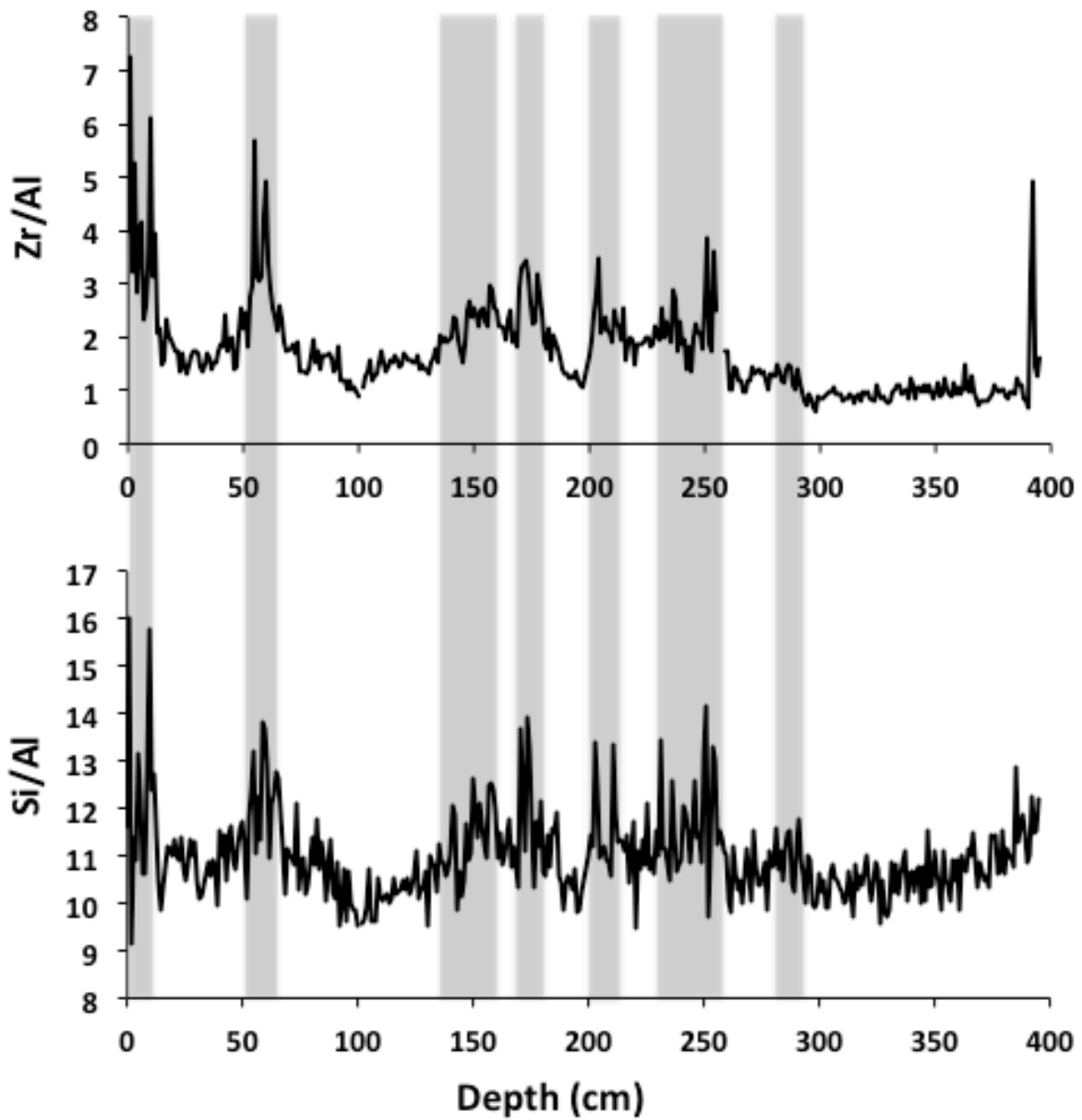
635 with the clay and silt sediments below. **b)** Granulometric distribution of surface samples collected

636 on a E-W transect from the Sea and the Barrier (red) to the lagoon (blue). Evolution of the 160-  
637 653  $\mu\text{m}$  population from the sea to the lagoon in surface samples.



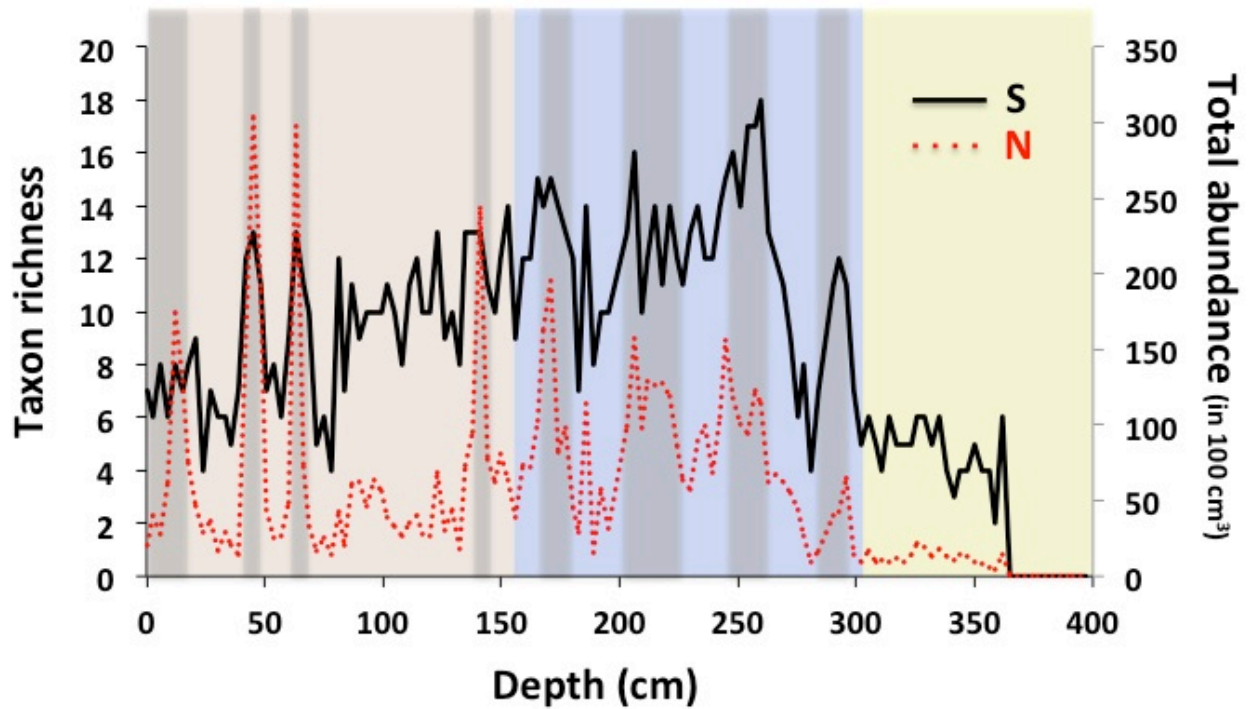
638  
639 **Figure 3.** Grain size population from the Mar Menor MM2 record with clay (<2  $\mu\text{m}$ ), silt (>2 and

640 <63  $\mu\text{m}$ ) and sand fraction (>63 $\mu\text{m}$ ). Shaded areas mark the main variations of the sand fraction.  
641



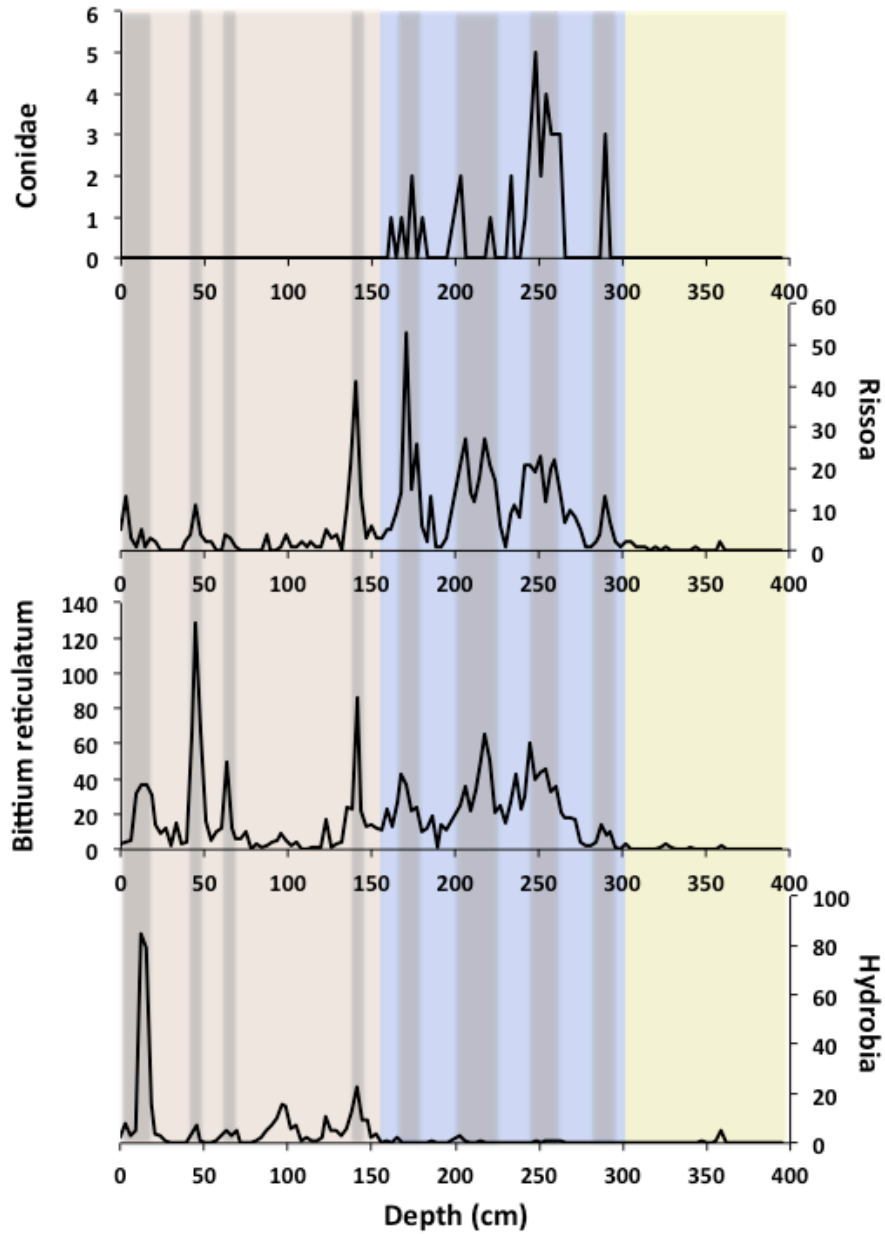
642  
643  
644  
645 **Figure 4.** XRF records from the core MM2 with down-core variations of ratio  $\text{Zr/Al}$  and  $\text{Si/Al}$ .  
646 Shaded areas mark the main variations of  $\text{Zr/Al}$  and  $\text{Si/Al}$ .

647  
648  
649  
650

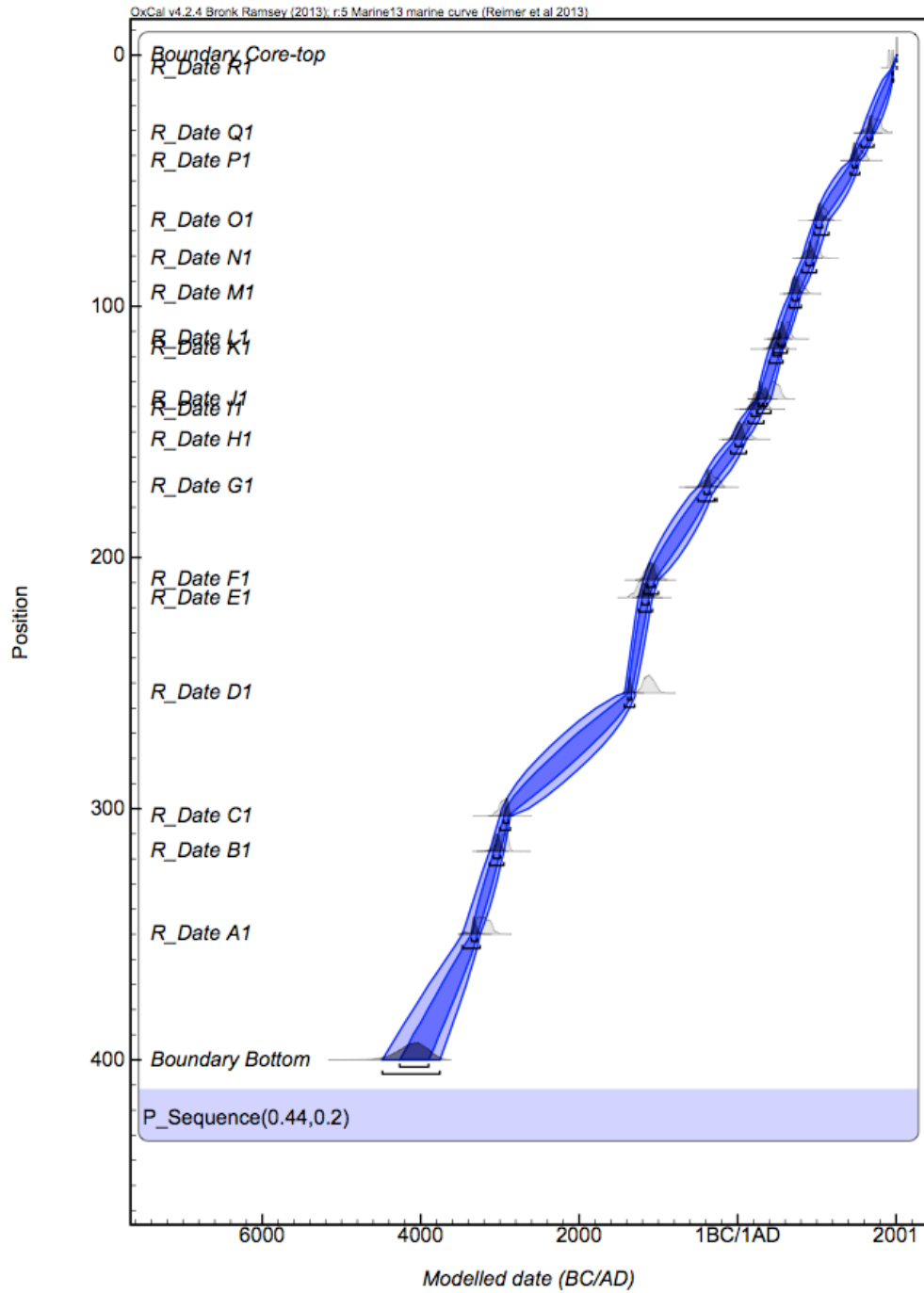


651  
652 **Figure 5.** Taxon richness (S) and total number of individuals (N) with depth from the core MM2.  
653 Macro-fauna samples were taken at fixed volume (100 cm<sup>3</sup>). The different colour bands  
654 correspond to depths: azoic (yellow), under higher marine influence (blue) and under a  
655 progressive isolation of the Mar Menor from the Mediterranean Sea (brown). The grey bands  
656 correspond to punctual peaks in species richness, probably related to episodes of rupture of the  
657 sandbar.  
658





659  
 660 **Figure 6.** Evolution of the abundance in mollusc population (number of individuals in 100 cm<sup>3</sup>)  
 661 with depth: lagoonal specie (*Hydrobia acuta*); typical marine specie (*Conus ventricosus*:  
 662 Conidae), marine influence (*Bittium Reticulatum* and *Pusillina lineolata*: Rissoa).  
 663  
 664

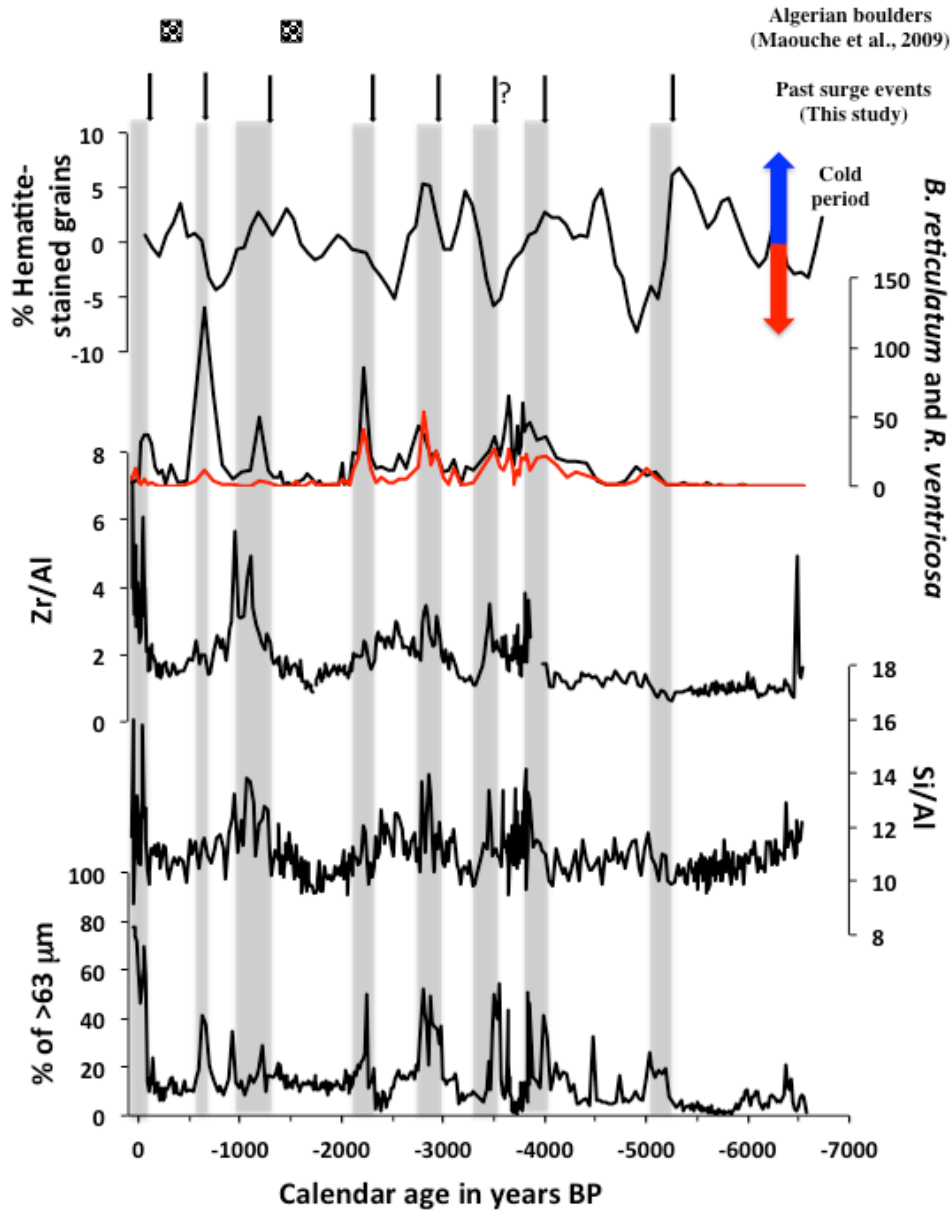


665

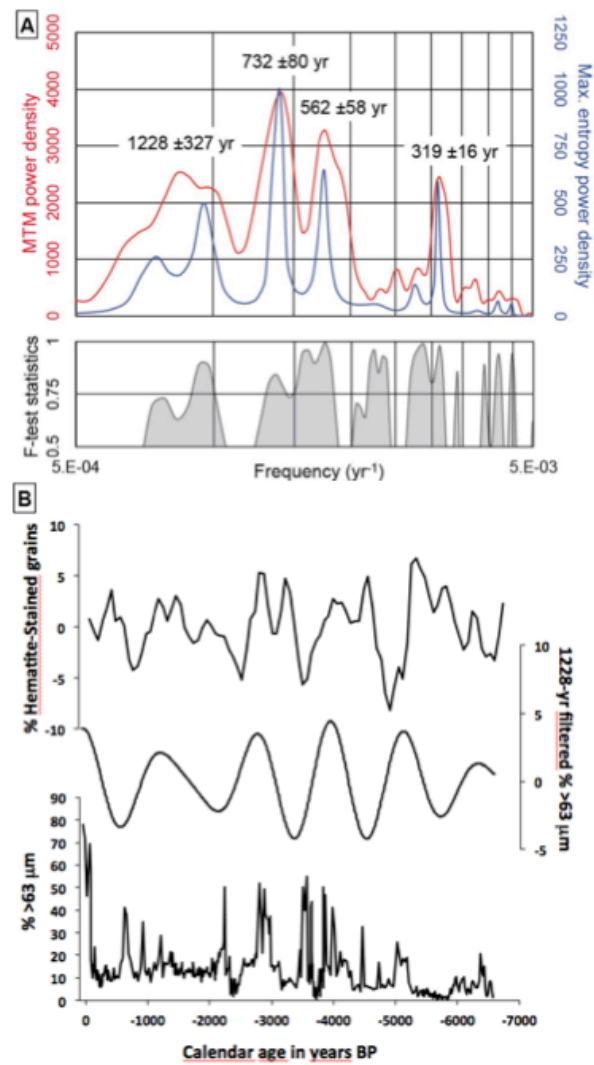
666 **Figure 7.** Age vs Depth for the core MM2. The Age model was calculated using OxCal 4 with 17

667 <sup>14</sup>C dates.

668



669  
 670  
 671 **Figure 8.** Core MM2 with from bottom to top: Grain size (sand fraction); Si/Al and Zr/Al XRF  
 672 ratio; number of *B. reticulatum* (Black line) and *R. Ventricosa* (Red line), % Hematite-stained  
 673 grains (Bond et al., 1997, 2001), ages of Algerian boulders (Maouche et al., 2009). Grey bands  
 674 are the past surge events.  
 675



677

678 **Figure 9.** Time series analysis from the Mar Menor MM2 record. (A) Spectral analyses of the %  
 679 of sand with AnalySeries v.2.0.8 (Paillard et al., 1996) by using the Multi-Taper method (linear  
 680 trend removed, width.ndata product: 1.3; number of windows: 2) and the Maximum entropy  
 681 method (linear trend removed, % of series: 40, number of lags: 133). (B) Comparison between  
 682 the % Hematite-stained grains (Bond et al., 1997, 2001), the Gaussian filter on the % of sand for  
 683 the 1228-yr period (frequency: 0.0008, bandwidth: 0.0002) and the sand fraction of the core  
 684 MM2.

685